

• 临床研究 •

基于压缩感知3D-SPACE序列对喙锁韧带的解剖学定量研究

王梦悦, 赵如盛, 徐磊*

南京医科大学第一附属医院放射科, 江苏 南京 210029

[摘要] 目的: 使用三维可变翻转角快速自旋回波(three-dimensional sampling perfection with application optimized contrast using different flip angle evolution, 3D-SPACE)序列联合压缩感知(compressed sensing, CS)技术, 在健康人群中定量测量喙锁韧带的两个组成部分, 斜方韧带与锥状韧带各自的长度、附着点宽度、附着点位置等解剖学参数。方法: 收集无肩部外伤行肩关节磁共振(magnetic resonance imaging, MRI)检查的志愿者64例, 进行冠状位T1加权像(T1-weighted image, T1WI)3D CS-SPACE序列的扫描。两名放射科医师分别对图像进行多平面重建, 在斜冠状位图像上测量斜方韧带与锥状韧带的长度、锁骨上附着处宽度以及附着处中心点距锁骨外侧缘的距离, 在斜矢状位图像上测量两者在喙突上附着处宽度, 在斜轴位图像上测量斜方韧带与锥状韧带在喙突附着处中心点距喙突外侧缘的距离以及喙突的大小。当两名医师测量结果具有一致性时, 取平均值用于统计学分析。按性别分组, 比较各参数组间一致性, 并将喙锁韧带各解剖定量数据与年龄、喙突大小进行相关性分析。结果: 斜方韧带长度、在锁骨及喙突上的附着处宽度、附着处中心点距锁骨、喙突外侧缘的距离以及锥状韧带附着处中心点距锁骨、喙突外侧缘的距离在男女组间的差异均有统计学意义(P 均 < 0.05)。年龄与各解剖参数间均不具有相关性(P 均 > 0.05)。除锥状韧带长度外, 其余斜方韧带及锥状韧带解剖学定量参数均与喙突大小具有不同程度的相关性(P 均 < 0.05)。结论: 3D CS-SPACE序列能够清晰显示斜方韧带与锥状韧带的解剖学结构, 通过其获得斜方韧带与锥状韧带的定量解剖学参数, 为肩锁关节损伤患者的个体化手术治疗提供依据, 有利于减少并发症。

[关键词] 喙锁韧带; 斜方韧带; 锥状韧带; 磁共振成像; 压缩感知; 解剖

[中图分类号] R322.73; R684

[文献标志码] A

[文章编号] 1007-4368(2025)11-1634-07

doi: 10.7655/NYDXBNSN250924

Anatomical quantitative study of coracoclavicular ligament using 3D-SPACE sequence based on compressed sensing

WANG Mengyue, ZHAO Rusheng, XU Lei*

Department of Radiology, the First Affiliated Hospital of Nanjing Medical University, Nanjing 210029, China

[Abstract] **Objective:** Using the three-dimensional sampling perfection with application optimized contrast using different flip angle evolution (3D-SPACE) sequence combined with compressed sensing (CS) technology, the anatomical parameters of the trapezoid ligament and the conoid ligament (the two components of the coracoclavicular ligament), such as the length, the attachment footprint width, and the position of attachment footprint center, were quantitatively measured in a healthy population. **Methods:** Sixty-four volunteers without shoulder trauma who underwent shoulder joint magnetic resonance imaging (MRI) examination were enrolled. The coronal T1-weighted image (T1WI) 3D CS-SPACE sequence scans were performed on them. Two radiologists performed multiplanar reconstruction on these images, measuring the length of the trapezoid and conoid ligaments, the attachment footprint width on the clavicle, and the distance from the attachment footprint center to the outer edge of the clavicle on the oblique coronal image. The attachment footprint width on the coracoid process was measured on the oblique sagittal image. The distance from the attachment footprint center of these two ligaments to the outer edge of the coracoid process and the size of the coracoid process were measured on the oblique axial image. When the measurement results of two physicians were consistent, the average was taken for statistical analysis. Volunteers were grouped by sex, the consistency of each parameter was compared, and the correlation between anatomical quantitative data of the coracoclavicular ligament and age or coracoid process size was analyzed. **Results:** The length of the trapezoid ligament, the

[基金项目] 国家自然科学基金(62071216)

*通信作者(Corresponding author), E-mail: xulei900427@163.com (ORCID: 0000-0002-0223-9010)

attachment footprint width on the clavicle and coracoid process of the trapezoid ligament, the distance from attachment footprint center of the trapezoid ligament to the outer edge of the clavicle and coracoid process, and the distance from attachment footprint center of the conoid ligament to the outer edge of the clavicle and coracoid process all showed statistical differences between males and females (all $P < 0.05$). There was no correlation between age and various anatomical parameters (all $P > 0.05$). Except for the length of the conoid ligament, the anatomical quantitative parameters of the trapezoid ligament and conoid ligament exhibited varying degrees of correlation with the size of the coracoid process (all $P < 0.05$). **Conclusion:** The 3D CS-SPACE sequence clearly displays the anatomical structures of the trapezoid ligament and conoid ligament, and obtains quantitative anatomical parameters of them, providing a basis for individualized surgical treatment of patients with acromioclavicular joint injuries and reducing the occurrence of complications.

[Key words] coracoclavicular ligament; trapezoid ligament; conoid ligament; magnetic resonance imaging; compressed sensing; anatomy

[J Nanjing Med Univ, 2025, 45(11): 1634-1640]

肩锁关节损伤的发生率因交通事故、运动损伤等增加,占全部肩关节损伤的9%~12%^[1-2]。肩锁关节损伤的处理方法目前暂未统一,但普遍认为损伤分级为Rockwood IV~VI级的患者,临床需要进行手术治疗^[3],其中喙锁韧带的解剖学重建至关重要^[4-5]。喙锁韧带由前外侧的斜方韧带及后内侧的锥状韧带组成^[6-7],目前喙锁韧带的定量解剖研究多在干燥尸体上进行^[8],或在健康人群中使用常规磁共振成像(magnetic resonance imaging, MRI)序列测量^[2],未具体区分斜方韧带与锥状韧带,较少对健康人群的斜方韧带及锥状韧带分别进行定量解剖测量。

三维可变翻转角快速自旋回波序列(three-dimensional sampling perfection with application optimized contrast using different flip angle evolution, 3D-SPACE)通过体积激励在相位编码的z轴方向上可以产生比二维图像更薄的切片,同时联合压缩感知(compressed sensing, CS)技术,实现了在较短的扫描时间内,获得可以在任意切面方向上多平面重建的3D图像。本课题组前期研究已经证实3D CS-SPACE序列对于肩锁关节损伤患者的韧带损伤程度的诊断具有较高价值^[9],相比常规二维快速自旋回波(turbo spin echo, TSE)序列T1加权像(T1-weighted image, T1WI)和质子密度加权像(proton density weighted image, PdWI),能够有效分辨斜方韧带与锥状韧带,在较短的扫描时间内获得清晰的图像,为患者的临床损伤Rockwood分级及后续的临床治疗方案提供帮助。因此,本研究旨在使用3D CS-SPACE序列,在健康人群中定量测量斜方韧带与锥状韧带的长度、附着点宽度、附着点位置等解剖学参数,为之后的肩锁关节损伤患者的个性化手术治疗提供相应的解剖学依据,以更好地恢复肩锁关节

功能,降低并发症的发生率。

1 对象和方法

1.1 对象

收集2023年7月—2025年3月在南京医科大学第一附属医院就诊的无肩部外伤行肩关节MRI检查的志愿者64例,年龄(52.5±14.5)岁。其中男26例,(49.6±15.4)岁;女38例,(54.4±15.3)岁。纳入标准:①发育正常的成年人;②无肩部外伤史及手术史。排除标准:①肩部肿瘤史;②类风湿性关节炎等结缔组织疾病;③图像质量不合格。本研究经南京医科大学第一附属医院伦理委员会批准(2023-SR-700),所有受检者均已签署知情同意书。

1.2 方法

1.2.1 MRI检查方法

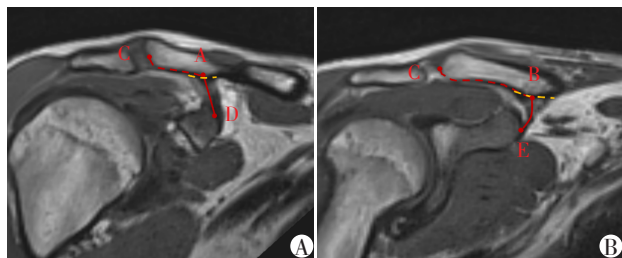
所有扫描均采用西门子Vida 3.0T超导型MRI和12通道相控阵肩部专用线圈,体位与常规二维MRI扫描保持一致,采用仰卧位,头先进,受检手臂置于身体一侧,掌心向内并采用沙袋对患者上肢进行固定。所有患者均进行3D CS-SPACE冠状位的T1WI序列图像采集,其扫描线平行于肩胛骨喙突与肱骨小结节之间的连线。

冠状位的T1WI 3D CS-SPACE序列扫描参数如下:重复时间(repetition time, TR)设置为400 ms,回波时间(echo time, TE)为21 ms,视野(field of view, FOV)为220 mm×220 mm,层厚为1.0 mm,层间距为0 mm,采集矩阵为224 mm×224 mm,加速因子为3,研究中该序列平均扫描时间为217 s。

1.2.2 斜冠状位图像喙锁韧带定量数据的测量

由2名具有5年以上肌骨系统影像诊断工作经验的放射科医师分别在Carestream Vue PACS工作

站上对斜冠状位图像进行数据测量。要求2人对扫描所得冠状位T1WI 3D CS-SPACE序列图像进行多平面重建,选取斜方韧带及锥状韧带显示最清晰的斜冠状位图像。分别标记:斜方韧带于锁骨附着处的中心点(点A);锥状韧带于锁骨附着处的中心点(点B);锁骨外侧边缘中心点(点C);斜方韧带于喙突附着处的中心点(点D);锥状韧带于喙突附着处的中心点(点E)。分别测量:斜方韧带锁骨附着处中心点与喙突附着处中心点之间的距离,评估斜方韧带长度(AD);锥状韧带锁骨附着处中心点与喙突附着处中心点之间的距离,评估锥状韧带长度(BE);斜方韧带锁骨附着处中心点至锁骨外侧缘中心距离(AC);锥状韧带锁骨附着处中心点至锁骨外侧缘中心距离(BC);斜方韧带于锁骨附着处宽度(width on the clavicle of the trapezoid ligament, TLW);锥状韧带于锁骨附着处宽度(width on the clavicle of the conoid ligament, CLW)(图1)。



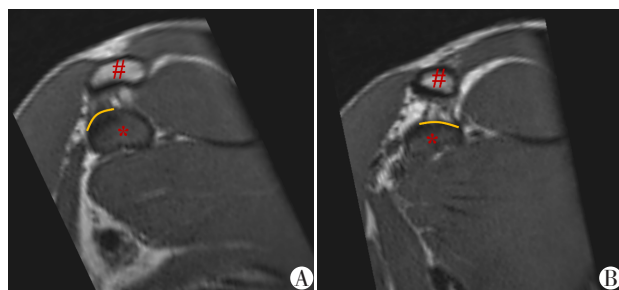
A: Optimal oblique coronal view of the trapezoid ligament. The red solid line represents the length of the trapezoid ligament (AD), the red dashed line represents the distance from the attachment footprint center of the trapezoid ligament to the outer edge of the clavicle (AC), and the yellow dashed line represents the attachment footprint width on the clavicle of the trapezoid ligament (TLW). B: Optimal oblique coronal view of the conoid ligament. The red solid line represents the length of the conoid ligament (BE), the red dashed line represents the distance from the attachment footprint center of the conoid ligament to the outer edge of the clavicle (BC), and the yellow dashed line represents the attachment footprint width on the clavicle of the conoid ligament (CLW).

图1 斜冠状位图像喙锁韧带定量数据的测量

Figure 1 Quantitative data measurement of coracoclavicular ligament on oblique coronal images

1.2.3 斜矢状位图像喙锁韧带定量数据的测量

对扫描所得的冠状位T1WI 3D CS-SPACE序列图像进行多平面重建,选取斜方韧带及锥状韧带显示最清晰的斜矢状位图像,分别测量斜方韧带于喙突附着处宽度(width on the coracoid process of the trapezoid ligament, TLD)和锥状韧带于喙突附着处宽度(width on the coracoid process of the conoid ligament, CLD)(图2)。



A: Optimal oblique sagittal view of the trapezoid ligament. #represents clavicle, *represents coracoid process, and the yellow solid line represents the attachment footprint width on the coracoid process of the trapezoid ligament (TLD). B: Optimal oblique sagittal view of the conoid ligament. #represents clavicle, *represents coracoid process, and the yellow solid line represents the attachment footprint width on the coracoid process of the conoid ligament (CLD).

图2 斜矢状位图像喙锁韧带定量数据的测量

Figure 2 Quantitative data measurement of coracoclavicular ligament on oblique sagittal images

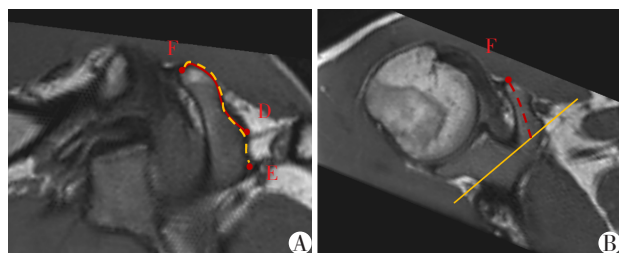
1.2.4 斜轴状位图像定量数据的测量

扫描所得的冠状位T1WI 3D CS-SPACE序列图像进行多平面重建,分别标记:斜方韧带于喙突附着处的中心点(点D);锥状韧带于喙突附着处的中心点(点E);喙突外侧边缘中心点(点F)。分别测量:斜方韧带喙突附着处中心点至喙突外侧缘的距离(DF);锥状韧带喙突附着处中心点至喙突外侧缘距离(EF)。选取喙突显示最清晰的斜轴状位图像,于喙突与关节盂之间切迹处,作一条平行于关节盂的切线。由喙突远端中心点沿喙突长轴方向画线至与该平行线交点处,评估喙突大小(size of coracoid process, CPL)(图3)。

1.3 统计学方法

使用SPSS27.0软件进行统计学分析,将2名肌骨诊断放射科医师的测量结果进行一致性检验,当两组数据具有一致性时,取两组数据平均值用于下一步数据分析。

以性别作为分组依据,对所有分组数据进行正态性检验,对于符合正态分布的计量资料采用均数±标准差($\bar{x} \pm s$)表示,若方差齐则进行t检验评估男女组别间数据的一致性,若方差不齐则进行校正的t'检验。对于不符合正态分布的计量资料采用中位数(四分位数) $[M(P_{25}, P_{75})]$ 表示,并进行两独立样本Wilcoxon秩和检验评估一致性。相关性分析采用Pearson相关分析及Spearman相关分析,评估喙锁韧带解剖定量数据与年龄、喙突大小之间的关系。 $P < 0.05$ 为差异有统计学意义。



A: The red solid line represents the distance from the attachment footprint center of the trapezoid ligament to the outer edge of the coracoid process (DF), and the yellow dashed line represents the distance from the attachment footprint center of the conoid ligament to the outer edge of the coracoid process (EF). B: The red dashed line represents the size of coracoid process (CPL).

图3 斜轴位图像喙锁韧带定量数据的测量

Figure 3 Quantitative data measurement of coracoclavicular ligament on oblique axial images

2 结果

2名肌骨诊断放射科医师的测量结果均具有一致性($P > 0.05$),以2名医师测量数据平均值用于下一步数据分析。以性别作为分组依据,锥状韧带长度(BE)、锥状韧带于锁骨附着处宽度(CLW)及锥状韧带于喙突附着处宽度(CLD)差异均无统计学意义(P 均 > 0.05),其余斜方韧带与锥状韧带解剖学定量测

量数据组间差异均有统计学意义(P 均 < 0.05 ,表1)。

将年龄及喙突大小(CPL)分别与斜方韧带及锥状韧带解剖学各定量测量数据进行相关性分析,年龄与各解剖参数间均不具有相关性(P 均 > 0.05)。喙突大小(CPL)与锥状韧带长度(BE)之间不具有相关性($P > 0.05$),与斜方韧带及锥状韧带锁骨附着处中心点至锁骨外侧缘中心距离(AC、BC)、斜方韧带及锥状韧带于锁骨附着处宽度(TLW、CLW)具有弱相关性,与斜方韧带长度(AD)、斜方韧带及锥状韧带喙突附着处中心点至喙突外侧缘的距离(DF、EF)、斜方韧带及锥状韧带于喙突附着处宽度(TLD、CLD)具有中等相关性(表2)。

3 讨论

肩锁关节损伤在肩部损伤中常见,主要发生于肩部的直接撞击,或在摔倒时由手臂伸直时的间接作用力造成^[1,10]。对于肩锁关节的损伤程度,使用Rockwood分类方法^[10-11]。Rockwood I级与II级患者,普遍认为不需要进行手术治疗,只需要保守治疗即可。Rockwood III级患者是否需要手术治疗,目前仍存在争议^[12]。而Rockwood IV~VI级患者,则推荐进行手术复位与固定^[11,13-14]。肩锁关节

表1 斜方韧带及锥状韧带各解剖学定量参数在不同性别间的一致性

Table 1 Consistency of anatomical quantitative parameters of the trapezoid ligament and conoid ligament across sexes

Parameter	Female(n=38)	Male(n=26)	t/t'/Z	P
AD(mm, $\bar{x} \pm s$)	15.18 \pm 1.75	16.72 \pm 1.64	-3.552	<0.001
BE(mm, $\bar{x} \pm s$)	11.27 \pm 1.41	11.42 \pm 1.33	-0.386	0.701
AC(mm, $\bar{x} \pm s$)	19.71 \pm 1.71	21.25 \pm 2.40	-2.820	0.007
BC(mm, $\bar{x} \pm s$)	34.27 \pm 2.22	36.23 \pm 3.60	-2.480	0.018
TLW(mm, $\bar{x} \pm s$)	11.79 \pm 1.32	12.63 \pm 1.36	-2.472	0.016
CLW[mm, $M(P_{25}, P_{75})$]	10.07(9.82, 10.74)	10.94(9.75, 11.78)	-1.934	0.053
DF(mm, $\bar{x} \pm s$)	30.16 \pm 4.30	34.66 \pm 3.94	-4.250	<0.001
EF(mm, $\bar{x} \pm s$)	33.63 \pm 4.41	38.12 \pm 3.34	-4.393	<0.001
TLD(mm, $\bar{x} \pm s$)	10.90 \pm 0.79	11.38 \pm 0.99	-2.150	0.035
CLD(mm, $\bar{x} \pm s$)	10.02 \pm 1.49	10.51 \pm 1.27	-1.351	0.182
CPL(mm, $\bar{x} \pm s$)	23.53 \pm 2.80	25.85 \pm 2.91	-3.200	0.002

表2 斜方韧带及锥状韧带各解剖学定量参数与年龄、喙突大小的相关性分析

Table 2 Correlation analysis of anatomical quantitative parameters of the trapezoid ligament and conoid ligament with age and coracoid process size

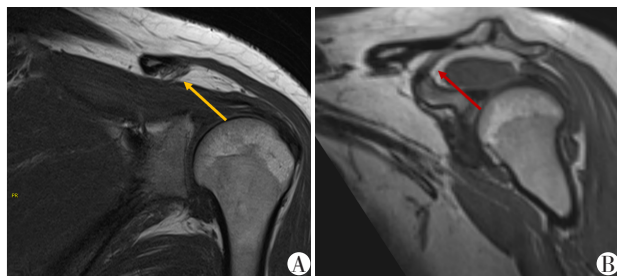
Factor		AD	BE	AC	BC	TLW	CLW	DF	EF	TLD	CLD
Age	r	0.153	-0.077	-0.193	-0.006	0.159	0.019	0.197	0.174	-0.018	0.032
	P	0.229	0.543	0.126	0.963	0.209	0.884	0.119	0.169	0.890	0.800
CPL	r	0.512	0.200	0.354	0.333	0.387	0.391	0.572	0.570	0.702	0.686
	P	<0.001	0.113	0.004	0.007	0.002	0.001	<0.001	<0.001	<0.001	<0.001

手术治疗主要包括克氏针复位、Bosworth螺钉固定、Weaver-Dunn手术、Endobutton钢板手术、关节镜下Endobutton重建喙锁韧带治疗、关节镜下TightRope喙锁韧带重建技术等^[3,11],有研究证实解剖学重建技术在生物力学上优于非解剖学重建技术^[4-5],其中改善喙锁韧带的结构对优化肩部生物力学功能至关重要^[1,12]。为了准确重建喙锁韧带,需要在锁骨及喙突上创建骨隧道,因此准确了解喙锁韧带附着区域的正确解剖学定量参数对手术中正确重建喙锁韧带是必要的,而位置不当的骨隧道则会增加并发症发生风险^[4-5]。

喙锁韧带为肩锁关节外韧带,是连接锁骨与喙突之间的韧带复合体,两者形成“V”字结构,共同悬吊肩锁关节,为肩锁关节的垂直方向运动提供稳定性^[7,15-16]。喙锁韧带由前外侧的斜方韧带及后内侧的锥状韧带组成^[6]。斜方韧带由喙突基底前外侧缘走行至锁骨外下方,呈斜方形,可防止肩锁关节向后、旋转移位。锥状韧带呈锥形,由喙突基底内侧螺旋走行至锁骨外1/3的中下方,主要防止肩锁关节向上、向前及螺旋移位^[6-7,17]。因此,在手术中不应将两者视为一个结构。

常规肩关节二维MRI扫描时间较长,易产生运动伪影,而3D CS-SPACE序列能够在相对较短的扫描时间内,获得层厚更薄、质量更高的图像,且已在颅内强化病变、脑血管壁、脑静脉窦、膝关节及肩关节等部位应用^[18-23]。前期本课题组对肩锁关节外伤患者的研究发现,对外伤患者进行肩锁关节Rockwood分级,3D CS-SPACE序列较常规二维MRI序列具有更高的诊断价值^[9],能够清晰显示斜方韧带与锥状韧带解剖结构。而二维MRI扫描序列图像层较厚,无法有效区分斜方韧带及锥状韧带。同时,由于二维MRI图像无法进行多平面重建,在测量中更易发生测量误差甚至无法测量(图4)。

本研究在获得T1WI 3D CS-SPACE序列图像后,通过多平面重建,测量斜方韧带与锥状韧带的长度、附着点位置及附着点宽度等多项解剖学定量参数,发现不同性别的斜方韧带长度(AD)、斜方韧带与锥状韧带于锁骨附着处中心点至锁骨外侧缘中心距离(AC、BC)、斜方韧带与锥状韧带于喙突附着处中心点至喙突外侧缘中心距离(DF、EF)、斜方韧带于锁骨及喙突附着处宽度(TLW、TLD)差异均有统计学意义,且男性各解剖参数均值均高于女性,这与Xue等^[8]测量的结果一致,原因可能是男性平均身高较女性高,男性解剖结构间的距离更大,



A: 2D T1WI coronal image, with yellow arrow showing the footprint of the trapezoid ligament at the clavicle but failing to simultaneously display the distal clavicle, making it impossible to measure the distance from the attachment footprint center to the outer edge of the clavicle. B: 3D CS-SPACE T1WI image, with red arrows showing the complete course and attachment of the trapezoid ligament after multiplanar reconstruction, which can be used to measure various anatomical parameters.

图4 2D T1WI冠状位图像与3D CS-SPACE图像对比

Figure 4 Comparison between 2D T1WI coronal image and 3D CS-SPACE image

使解剖定量参数测量值更大。这也与本研究中男性喙突大小(CPL)较女性更大相符。因此,建议对于身高更高的肩锁关节损伤患者,在重建喙锁韧带解剖时,应采用更长的喙锁韧带重建长度,选取更合适的骨隧道建立位置。而锥状韧带的走行较斜方韧带更为短直,纤维束相对聚集,这可能是导致锥状韧带长度(BE)及其于锁骨、喙突附着处宽度(CLW、CLD)差异无统计学意义的原因。

本研究中男、女斜方韧带长度(AD)分别为 (16.72 ± 1.64) mm、 (15.18 ± 1.75) mm,较Xue等^[8]测量的 (12.8 ± 2.7) mm更长,这可能是由于斜方韧带在斜冠状位上较宽,其内侧缘及外侧缘长度部分差异较大,而本研究选取了韧带附着点中央进行测量,产生了误差。而本研究中男、女锥状韧带的长度(BE)分别为 (11.42 ± 1.33) mm、 (11.27 ± 1.41) mm,与Xue等^[8]测量的 (11.2 ± 2.5) mm大致相仿。同时,本研究中斜方韧带与锥状韧带于锁骨、喙突上的附着处中心点距锁骨、喙突边缘的距离、附着宽度等也与既往测量结果大致相仿^[8,24-26],证实了3D CS-SPACE序列的图像质量高。

研究结果显示,斜方韧带及锥状韧带各项解剖学定量参数均与年龄没有明显相关性。本研究缺乏对患者身高信息的采集,因此采用测量喙突大小(CPL)的方法进行补充,结果显示大多数斜方韧带及锥状韧带解剖学定量参数均与喙突大小(CPL)具有不同程度的相关性。这一结论与男性患者的各项参数值较女性更大的结果相互印证,证实不同身高及骨架大小的患者,重建斜方韧带及喙锁韧带时

需要有所差别,这样更有利于对肩锁关节损伤患者的个体化治疗,帮助患者恢复功能。

本研究仍存在一定局限性。首先,本研究未能获得斜方韧带与锥状韧带的外翻角及后倾角的统计学参数^[26]。由于每个人锁骨及喙突走行及形态具有一定差异性,本研究未能确定合适的参考线用于测量角度,使得研究者间的差异性较大。其次,斜方韧带及锥状韧带在锁骨及喙突上的附着处是一个平面,而本研究将附着处简化为线样附着,仅测量了两者与锁骨、喙突长轴平行的附着面积,而并没有测量与锁骨、喙突长轴垂直方向上的附着宽度,将三维的韧带简化为二维结构,存在一定的局限性。

综上所述,3D CS-SPACE序列能够清晰显示斜方韧带与锥状韧带的解剖学结构,通过其获得斜方韧带与锥状韧带的定量解剖学参数,可为肩锁关节损伤患者的个体化手术治疗提供依据。

利益冲突声明:

所有作者声明不存在利益冲突。

Conflict of Interests:

All authors declare that there is no conflict of interests.

作者贡献声明:

王梦悦收集、整理、分析数据,撰写文章初稿;王梦悦、徐磊分别测量数据;赵如盛对患者进行MRI扫描,采集图像;徐磊设计研究方案,对稿件重要内容进行审阅和修改。

Author's Contributions:

WANG Mengyue collected, sorted, and analyzed the data, and wrote the first draft of the article; WANG Mengyue and XU Lei measured the data separately; ZHAO Rusheng conducted MRI examinations on the patients and collected images; XU Lei designed the research plan, reviewed the important contents and revised the manuscript.

[参考文献]

- [1] LYLE C E, PARKER D. Open anatomic coracoclavicular ligament reconstruction for acromioclavicular joint injuries[J]. *Clin Sports Med*, 2023, 42(4): 589-598
- [2] 张磊,张华强,金玉峰,等. 基于MRI喙锁韧带的解剖学参数分析[J]. *中国临床解剖学杂志*, 2022, 40(3): 259-262
ZHANG L, ZHANG H Q, JIN Y F, et al. Analysis on the anatomical parameters of coracoclavicular ligament based on MRI[J]. *Chinese Journal of Clinical Anatomy*, 2022, 40(3): 259-262
- [3] 徐科腾,梁远,王静成. 肩锁关节脱位治疗的最新进展[J]. *南京医科大学学报(自然科学版)*, 2020, 40(10): 1565-1570
XU K T, LIANG Y, WANG J C. Developments in the treatment of acromioclavicular dislocation[J]. *Journal of Nanjing Medical University(Natural Sciences)*, 2020, 40(10): 1565-1570
- [4] SIRCANA G, SACCOMANNO M F, MOCINI F, et al. Anatomic reconstruction of the acromioclavicular joint provides the best functional outcomes in the treatment of chronic instability[J]. *Knee Surg Sports Traumatol Arthrosc*, 2021, 29(7): 2237-2248
- [5] CHANG P S, MURPHY C P, WHALEN R J, et al. Surgical pearls and pitfalls for anatomic acromioclavicular/coracoclavicular ligament reconstruction [J]. *Clin Sports Med*, 2023, 42(4): 621-632
- [6] PERRY N P J, OMONULLAEVA N K, BACEVICH B M, et al. Acromioclavicular joint anatomy and biomechanics: the significance of posterior rotational and translational stability[J]. *Clin Sports Med*, 2023, 42(4): 557-571
- [7] FLORES D V, GOES P K, GÓMEZ C M, et al. Imaging of the acromioclavicular joint: anatomy, function, pathologic features, and treatment[J]. *Radiographics*, 2020, 40(5): 1355-1382
- [8] XUE C, SONG L J, LI X, et al. Coracoclavicular ligaments anatomical reconstruction: a feasibility study [J]. *Int J Med Robot*, 2015, 11(2): 181-187
- [9] 赵如盛,王梦悦,徐露露,等. 基于压缩感知的3D CS-SPACE序列在肩锁关节损伤诊断中的应用价值[J]. *南京医科大学学报(自然科学版)*, 2024, 44(9): 1250-1256
ZHAO R S, WANG M Y, XU L L, et al. Application value of 3D CS - SPACE sequence based on compressed sensing in the diagnosis of acromioclavicular joint injury [J]. *Journal of Nanjing Medical University(Natural Sciences)*, 2024, 44(9): 1250-1256
- [10] MINKUS M, WIENERS G, MAZIAK N, et al. The ligamentous injury pattern in acute acromioclavicular dislocations and its impact on clinical and radiographic parameters[J]. *J Shoulder Elbow Surg*, 2021, 30(4): 795-805
- [11] GUZMAN A J, RAYOS DEL SOL S, DELA RUEDA T, et al. Open acromioclavicular repair with a suture cerclage tensioning system: a case series[J]. *Cureus*, 2023, 15(1): e34018
- [12] HASSEBROCK J D, STOKES D J, CRAM T R, et al. Arthroscopic repair and reconstruction of coracoclavicular ligament[J]. *Clin Sports Med*, 2023, 42(4): 599-611
- [13] LAMPLLOT J D, SHAH S S, CHAN J M, et al. Arthroscopic-assisted coracoclavicular ligament reconstruction: clinical outcomes and return to activity at mean 6-year follow-up [J]. *Arthroscopy*, 2021, 37(4): 1086-1095
- [14] JOSHI A, BASUKALA B, SINGH N, et al. Arthroscopy-assisted all-suture coracoclavicular and acromioclavicular joint stabilization in acute acromioclavicular joint injuries[J]. *Arthrosc Tech*, 2021, 10(5): e1293-e1306

- [15] 章 异,赵 佳,罗 倩,等.能谱CT在急性肩锁关节脱位患者喙锁韧带损伤诊断中的意义[J].中国骨与关节杂志,2022,11(10):738-744
ZHANG Y,ZHAO J,LUO Q, et al. Diagnosis of coracoclavicular ligament injury in acute acromioclavicular dislocations by energy spectrum CT[J]. Chinese Journal of Bone and Joint, 2022, 11(10): 738-744
- [16] KURATA S,INOUE K,HASEGAWA H, et al. The role of the acromioclavicular ligament in acromioclavicular joint stability: a cadaveric biomechanical study [J]. Orthop J Sports Med, 2021, 9(2): 2325967120982947
- [17] MANTRIPRAGADA S, BHAGWANI S, PEH W C, et al. Acromioclavicular joint injuries: imaging and management [J]. J Med Imaging Radiat Oncol, 2020, 64(6): 803-813
- [18] YUN S Y,HEO Y J. Clinical feasibility of post-contrast accelerated 3D T1-sampling perfection with application-optimized contrasts using different flip angle evolutions (SPACE)with iterative denoising for intracranial enhancing lesions: a retrospective study[J]. Acta Radiol, 2024, 65(6):654-662
- [19] GUGGENBERGER K V, VOGT M L, SONG J W, et al. High-resolution magnetic resonance imaging visualizes intracranial large artery involvement in giant cell arteritis[J]. Rheumatology(Oxford), 2025, 64(2): 842-848
- [20] HAKIM A, KURMANN C, POSPIESZNY K, et al. Diagnostic accuracy of high-resolution 3D T2-SPACE in detecting cerebral venous sinus thrombosis[J]. AJNR Am J Neuroradiol, 2022, 43(6): 881-886
- [21] LEE S, LEE G Y, KIM S, et al. Clinical utility of fat-suppressed 3-dimensional controlled aliasing in parallel imaging results in higher acceleration sampling perfection with application optimized contrast using different flip angle evolutions MRI of the knee in adults[J]. Br J Radiol, 2020, 93(1112): 20190725
- [22] VAN DYCK P, SMEKENS C, ROELANT E, et al. 3D caipirinha space versus standard 2d tse for routine knee MRI: a large-scale interchangeability study [J]. Eur Radiol, 2022, 32(9): 6456-6467
- [23] HOU B W, LI Y T, XIONG Y, et al. Comparison of caipirinha-accelerated 3D fat-saturated-space MRI with 2D MRI sequences for the assessment of shoulder pathology [J]. Eur Radiol, 2022, 32(1): 593-601
- [24] PEEBLES L A, AMAN Z S, KRAEUTLER M J, et al. Qualitative and quantitative anatomic descriptions of the coracoclavicular and acromioclavicular ligaments: a systematic review[J]. Arthrosc Sports Med Rehabil, 2022, 4(4): e1545-e1555
- [25] TAKASE K. The coracoclavicular ligaments: an anatomic study[J]. Surg Radiol Anat, 2010, 32(7): 683-688
- [26] ZHU N F, RUI B Y, ZHANG Y L, et al. Anatomic study of coracoclavicular ligaments for reconstruction of acromioclavicular joint dislocations [J]. J Orthop Sci, 2016, 21(6): 749-752
- [收稿日期] 2025-08-18
(本文编辑:陈汐敏)

(上接第1633页)

- early subclinical myocardial impairment in patients with long COVID syndrome using two-dimensional speckle tracking technique [J]. Journal of Nanjing Medical University(Natural Sciences), 2024, 44(2): 185-190
- [17] MARZLIN N, HAYS A G, PETERS M, et al. Myocardial work in echocardiography[J]. Circ Cardiovasc Imaging, 2023, 16(2): e014419
- [18] GONZALEZ P, LOZANO P, ROS G, et al. Hyperglycemia and oxidative stress: an integral, updated and critical overview of their metabolic interconnections[J]. Int J Mol Sci, 2023, 24(11): 9352
- [19] LIMA J, MOREIRA N C S, SAKAMOTO-HOJO E T, et al. Mechanisms underlying the pathophysiology of type 2 diabetes: from risk factors to oxidative stress, metabolic dysfunction, and hyperglycemia[J]. Mutat Res Genet Toxicol Environ Mutagen, 2022, 874: 503437
- [20] SLETTENA C, PETERSON L R, SCHAFFER J E, et al. Manifestations and mechanisms of myocardial lipotoxicity in obesity[J]. J Intern Med, 2018, 284(5): 478-491
- [21] DROSATOS K, SCHULZE P C. Cardiac lipotoxicity: molecular pathways and therapeutic implications [J]. Curr Heart Fail Rep, 2013, 10(2): 109-121
- [22] CATURANO A, GALIERO R, VETRANO E, et al. Insulin-heart axis: bridging physiology to insulin resistance [J]. Int J Mol Sci, 2024, 25(15): 8369
- [23] ABEL E D, O'SHEA K M, RAMASAMY R, et al. Insulin resistance: metabolic mechanisms and consequences in the heart [J]. Arterioscler Thromb Vasc Biol, 2012, 32(9): 2068-2076
- [24] PAPAPOSTOLO S, KEARNS J, COSTELLO B T, et al. Comparison of pressure vs volume overload ventricular wall stress in patients with valvular heart disease [J]. J Am Coll Cardiol, 2024, 84(7): 635-644
- [收稿日期] 2025-04-07
(本文编辑:唐震)